Available online at www.sciencedirect.com
SCIENCE DIRECT®
Corrosion Science 47 (2005) 2883–2900
CORROSION SCIENCE
www.elsevier.com/locate/corsci

A photoelectrochemical investigation of conversion coatings on Mg substrates

L. Anicai [1], R. Masi, M. Santamaria *, F. Di Quarto

Dipartimento di Ingegneria Chimica dei Processi e dei Materiali, Università di Palermo, Viale delle Scienze, 90128 Palermo, Italy

Available online 25 August 2005

Abstract

The structure, morphology and composition of conversion coatings grown in stannate bath on pure Mg were studied using potential–time, polarization curves, X-ray diffraction, scanning electron microscopy and photocurrent spectroscopy. The coating is manly constituted by crystalline magnesium–tin hydroxide, whose morphology and distribution depends on the conversion bath composition and temperature. The photoelectrochemical investigation allowed to estimate the band gap value of $MgSn(OH)_6$ and flat band potential. A sketch of the metal/passive film/electrolyte junction formed during conversion on the metal substrate is reported to account for the overall photoelectrochemical behaviour.

Keywords: Conversion coating; Mg; Mixed hydroxide; Photocurrent spectroscopy

1. Introduction

Light metals-based metallic materials are widely used in various fields of electrical engineering, electronics, aeronautics and automotive industries. Depending on the

* Corresponding author. Tel.: +39 091 6567287; fax: +39 091 6567280.
E-mail address: santamaria@dicpm.unipa.it (M. Santamaria).
[1] Permanent address: Department of Environmental Protection and Technological Development, Petromservice SA, str.Gral Budisteanu 11 bis, Bucharest, Romania.

0010-938X/$ - see front matter
doi:10.1016/j.corsci.2005.05.033

applied surface treatments, various coating types may be formed having different applications as (a) coating layers with decorative–anticorrosive properties; (b) adherent pre-treatment layers for successive finishing; (c) in composite materials with special functional characteristics.

In the case of Mg and its alloys, potential advantages due to interesting properties such as low density, high thermal conductivity, good workability, easy recycling and bio-compatibility, are counteracted by their poor corrosion and wear resistance. Moreover, the high chemical reactivity of Mg and its alloys, if exposed to aqueous solutions or humid atmosphere, with formation of a poorly protective surface layer has detrimental effect on further processing of such alloys [1–4].

Previous investigations [3,5–8] have shown that the electrochemical behaviour of Mg electrodes is strongly dependent on the electrolyte involved as well as on its pH value. Thus, according to their characteristic effect, electrolytes may act as (i) strong passivators (e.g. fluorides, chromates); (ii) moderate passivators (e.g. hydroxides, carbonates, borates, phosphates); (iii) moderate corrosion stimulators (e.g. sulphates, nitrates) or (iv) strong pitting agents (e.g. chlorides, bromides).

Coating procedures in the case of Mg and Mg alloys involves chemical/electrochemical conversion to produce a superficial layer of substrate metal oxides, chromates, phosphates or other compounds that are chemically bonded to the surface. These coatings are usually applied to impart corrosion protection and a good paint base properties to the metal. Among the conversion treatments the most used are those based on CrO_3 or chromate solutions which however has proved to have a harmful effect on the environment and human health, so that, the development of less toxic processes becomes a necessity.

One ''clean'' candidate for substitution of chromate-based solutions is represented by stannate-based chemical conversion bath allowing the formation of a surface layer with protective characteristics [1,9–11]. According to [11] the formation of a 2–3 μm adherent layer of $MgSnO_3 \cdot 3H_2O$ is occurring in alkaline stannate solution used for at least 20 min at a relatively high temperature (around 82 °C). The film was found to be developed by a nucleation and growth process through an initial corrosion film existing on the substrate. Huo et al. [10] suggested the formation of $MgSnO_3 \cdot H_2O$ during chemical conversion in stannate solution for 60 min at 90 °C. The layer exhibited a porous structure that provided some advantage for adsorption during sensitization treatment prior to a second step involving electroless nickel plating.

According to this previous work, stannate-based chemical conversion baths represent a potential environmental friendly treatment both for Mg and its alloys, offering some advantages for anticorrosion treatment. In spite of these aspects, there are just few reported data regarding the composition, structure, morphology and development of the coating on Mg metal.

In this paper, we present experimental results pertaining to the physico-chemical characterization of stannate-based chemical conversion layers grown on Mg substrates, carried out by ex situ SEM and XRD techniques and in situ electrochemical and photoelectrochemical techniques.

2. Experimental

In order to perform experiments, 99.9% pure magnesium working electrodes have been used, as metallic foils (125–150 μm thickness) or rods (7 mm diameter), provided from Goodfellow. Mg foil electrodes have been covered with lacomit stopping off, or in the case of rod electrodes embedded in a Teflon cylinder and sealed with epoxy resin (Torr Seal Varian Ass.), leaving under investigation in solution exposure (after chemical conversion treatment) a constant geometrical area. Before immersion in chemical conversion electrolyte, electrode surfaces have been subjected to mechanical polishing with 600 and 1200 emery paper, followed by washing with acetone in an ultrasonic bath for 5 min. A pickling step was applied, using 250 ml l^{-1} HF solution (40% HF) for 30 s at room temperature, followed by rinsing with distilled water and drying.

To form chemical conversion layers, alkaline stannate solutions have been prepared, whose compositions and operating parameters are given in Table 1.

The development of the conversion coating has been followed by recording the open circuit potential–time response, involving a Zahner 6 IMe potentiostat, against a saturated calomel reference electrode (SCE). Gravimetric experiments have been performed to evaluate the mass weight, on a minimum of three specimens for each variant.

The morphology of the coatings after stannate treatments has been examined by scanning electron microscopy (SEM) using a Philips ESEM microscope equipped with energy dispersive X-ray (EDX) analysis facilities. The structure of the coatings has been determined by X-ray diffraction (XRD), using CuKα radiation.

To get more qualitative and quantitative information on the electronic properties of conversion coatings and the structure of metal/passive film/electrolyte interface, photocurrent spectroscopy (PCS) technique has been used. A three electrode cell, equipped with flat quartz windows, was used for PCS investigation. The monochromatic light in a quite large range of wavelengths, between 200 and 800 nm,

Table 1
Composition and operation conditions for stannate-based chemical conversion treatments on Mg electrode

No.	Composition	g l^{-1}	Operation conditions
1	NaOH	9.95	$T = 82 \pm 5$ °C
	$K_2SnO_3 \cdot 3H_2O$	49.87	$t = 30$–60 min
	$NaC_2H_3O_2 \cdot 3H_2O$	9.95	Stationary conditions
	$Na_4P_2O_7$	49.87	
	pH = 11.5–12.0		
2	NaOH	10	$T = 90 \pm 5$ °C
	$K_2SnO_3 \cdot 3H_2O$	50	$t = 60$ min
	$NaC_2H_3O_2 \cdot 3H_2O$	10	Moderate stirring
	pH = 11.5–12.0		

is provided through a lamp–UV/VIS–monochromator–mechanical chopper system coupled to a lock in amplifier (EG&G 7206). The chopping frequency was 13 Hz. Data have been acquired through an analog/digital interface to a desk computer and corrected for the quantum emission of the light source (lamp and monochromator). Thus, on the *y*-axis of photocurrent spectra, a photocurrent yield in arbitrary units is reported.

3. Results and discussion

3.1. Gravimetric, morphological and XRD study

To monitor the formation of chemical conversion layers, the evolution of open circuit potential, U_{OC}, in time has been recorded, as reported in Fig. 1. According to the figure, several stages may be identified during coating process. Thus, in the first minutes of immersion, the potential moves towards more negative values, suggesting a probable initial oxide surface layer dissolution and an active dissolution before starting the passivation process. After about 2–4 min of immersion, the potential rose quite sharply, indicating a modification of metal surface owing to a formation of a hydride and/or a progressive covering of the surface with conversion layer. After 30–35 min, a steady-state condition is reached as evidenced by the quasi-constant corrosion potential value, suggesting a quite complete conversion process over the macroscopic Mg substrate surface.

The coating mass has been evaluated by gravimetry, weighing the Mg specimens of constant geometrical surface before and after conversion process for different immersion times, as shown in Fig. 2. Thus, a coating mass of about 0.3–0.4 mg cm^{-2} may be attained for 30–60 min of conversion time.

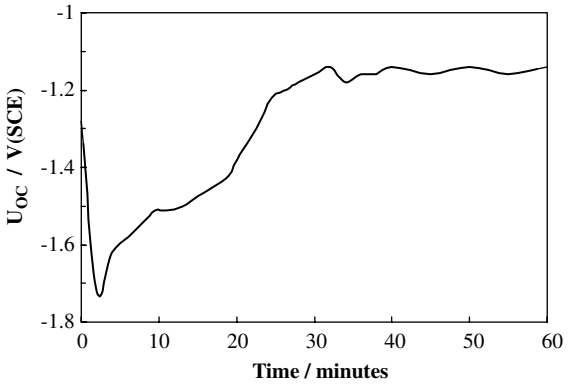

Fig. 1. Dependence of open circuit potential against immersion time during chemical conversion in stannate solution no. 1 for Mg electrode, at 82 °C.

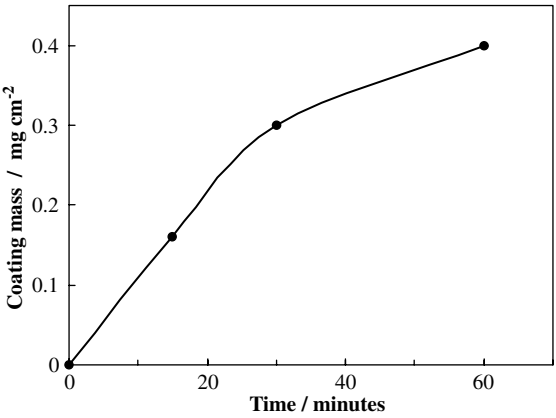

Fig. 2. The dependence of coating mass on immersion time, for a chemical conversion process in stannate solution no. 1, for Mg electrode, at 82 °C.

It should be mentioned that applying stannate solution no. 2, the conversion process occurs more slowly; the shape of open circuit potential in time is quite similar, but the quasi-constant value is attained after about 50–60 min of immersion.

The morphology of chemical conversion layers on Mg substrate for the two employed solutions are shown in Figs. 3 and 4. According to Fig. 3a, conversion layer formed in stannate solution no. 1 covers almost the entire substrate area as compared with solution 2, where uncovered areas of conversion layer may be found (see Fig. 4). The coating is formed by quite uniform spherical (see Fig. 3b) and cubic grains, respectively.

Analysis by EDX indicated that the coating grown in solution no. 1 was composed mainly by oxygen, magnesium and tin (with an atomic Mg/Sn ratio close to unity), with traces of sodium and phosphorus. The hydrogen contained in the coating was not detected by EDX.

Fig. 5 shows the XRD pattern for coated Mg substrates in the two different conversion solutions. Comparison of the patterns revealed several peaks characteristic to $MgSn(OH)_6$ for both applied variants. This result is at variance with other literature data [9,10], suggesting the formation of $MgSnO_3$ or $MgSnO_3 \cdot H_2O$, but agrees with data of Ref. [11]. For conversion layer grown in bath no. 2 some reflection in the XRD pattern suggests the possible presence of $Mg(OH)_2$ phase on the metal surface. Such a reflection, completely missing in the conversion layer grown in bath no. 1, is an indication that $Mg(OH)_2$ could also exist on this sample as a thin underlying layer covering the magnesium metal. The thicker and more compact conversion layer existing at the surface of the specimen converted in solution no. 1 could mask the small signal of the hydroxide although it cannot be excluded that in such specimen an amorphous hydroxide layer is formed. We will come back on this aspect in discussing the photoelectrochemical behaviour of the converted electrodes.

A preliminary electrochemical study based on potentiodynamic curves was undertaken on converted and unconverted Mg electrodes. In Fig. 6, we report in the Tafel

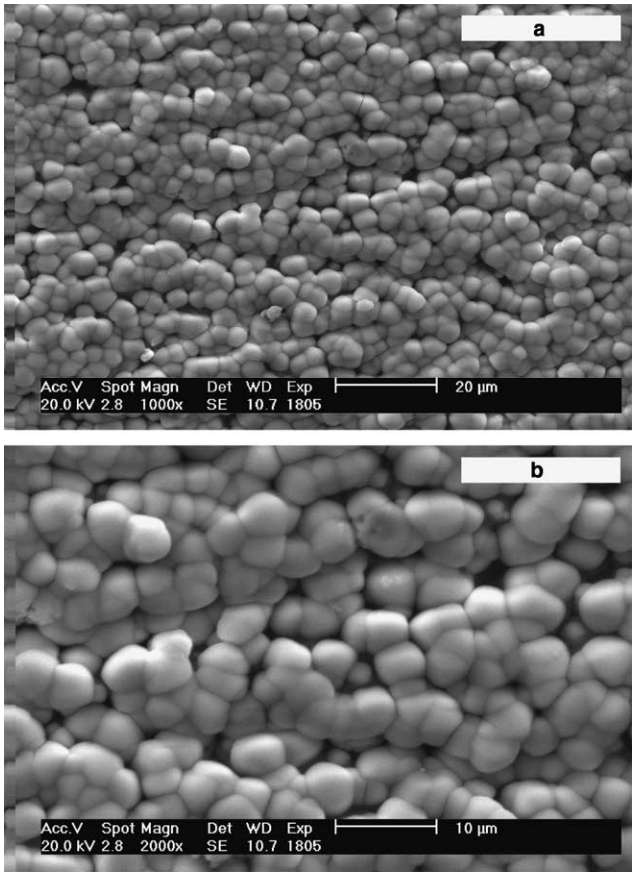

Fig. 3. SEM images showing the coating morphology of stannate-based conversion involving solution no. 1 for 30 min at 82 °C at different magnitudes.

plane the polarization curves recorded at 1 mV s^{-1} in 0.1 M NaOH at room temperature for Mg (a) after mechanical treatment, (b) after 30 min in 0.1 M NaOH at 82 °C and (c) after 30 min in solution no. 1 at 82 °C. In the absence of conversion layer, a cathodic Tafel line which accounts for the possible hydrogen evolution on oxidized Mg surface was recorded. The Tafel slopes for this cathodic process are 140 and 160 mV per current decade for electrode (a) and (b), respectively. This behaviour differs from that observed for the converted sample showing in a large range of cathodic potential values an almost constant current, typical of an electrochemical process under limiting current control.

A strongly different behaviour has been shown in the anodic branch. In fact, for Mg electrode as well as for Mg after immersion in hot NaOH for $U_E > U_{OC}$ an anodic current due the oxidation of magnesium to $Mg(OH)_2$ process has been detected, the lower value being measured for the second sample, whose surface is presumably

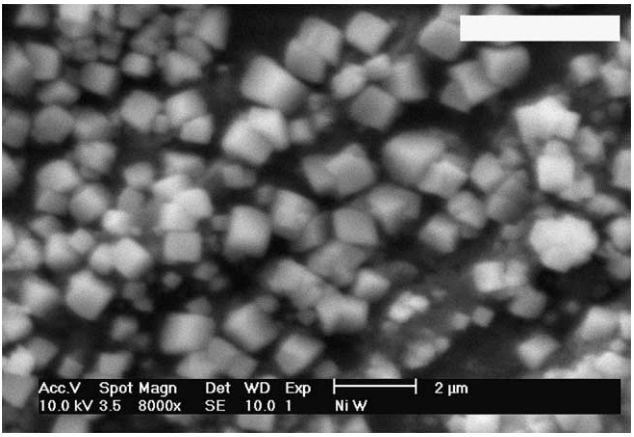

Fig. 4. SEM image showing the coating morphology of stannate-based conversion involving solution no. 2 for 60 min at 90 °C.

covered by the hydroxide before immersion in the polarizing electrolyte. In the case of converted sample, a very pronounced anodic peak is observed, sometimes followed by a second smaller anodic peak at higher potential before reaching a steady-state current density. The analysis of the polarizing curves of Fig. 6 clearly indicates that the differences in electrochemical behaviour of the electrodes must be attributed to the presence of stannate species in the electrolyte, derived from the selective dissolution of Sn(IV) of the conversion layer as SnO_3^{2-} ions, due the low stability of $Sn(OH)_4$ in alkaline environment [12]. According to Pourbaix, stannate ions may be reduced to bistannite ions. The rate of this process may be controlled by the diffusion of the stannate ions produced by the dissolution of the conversion layer, concentrated in the cavities between the spheres constituting the deposit. For polarizing voltage slightly higher than the corrosion potential $HSnO_2^-$ ions can be re-oxidized in the anodic branch, even if we cannot exclude that the measured anodic current is also due to the oxidation of magnesium from the uncoated areas. The second smaller anodic peak at higher potential can be attributed to the oxidation of adsorbed $HSnO_2^-$ ions.

It is important to stress that the red–ox reactions occurring during the polarization seem to interest only the surface of the conversion layer, since no appreciable differences in the morphology and structure of the film have been evidenced by SEM and XRD analysis after the polarization.

3.2. Photoelectrochemical study

To get more information on the electronic structure and, indirectly, on the chemical composition of chemical conversion layer grown in stannate solution, several photoelectrochemical experiments have been performed by recording the

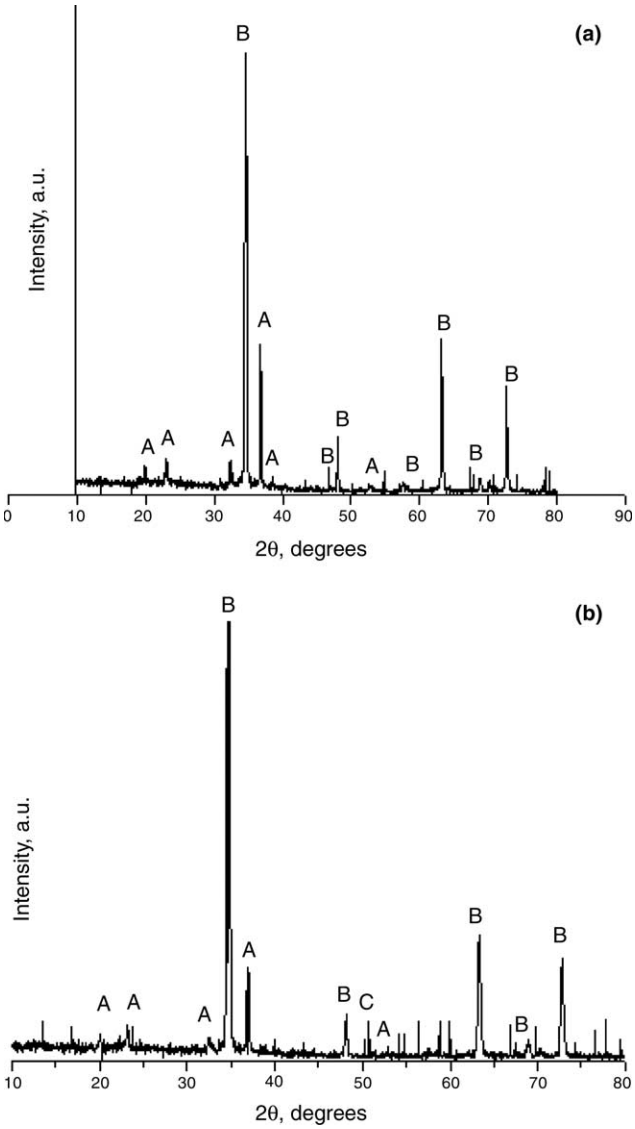

Fig. 5. XRD patterns of Mg electrode coated by chemical conversion layer involving: (a) solution no. 1 (30 min, 82 °C) and (b) solution no. 2 (60 min, 90 °C). Identification according to cards nos. 7-239 and 9-27 of JCPDS—International Centre for Diffraction Data. A: $MgSn(OH)_6$; B: Mg; C: $Mg(OH)_2$.

photocurrent spectra (I_{ph}–λ), at different constant electrode potentials, as well as the I_{ph} vs U_E plots (photocharacteristics) at a fixed wavelength.

Taking into account the previous results, pertaining to the morphology of the conversion layer, it can be considered that a chemical conversion process of 30 min in solution no. 1 and at least 60 min in solution no. 2 allows the formation

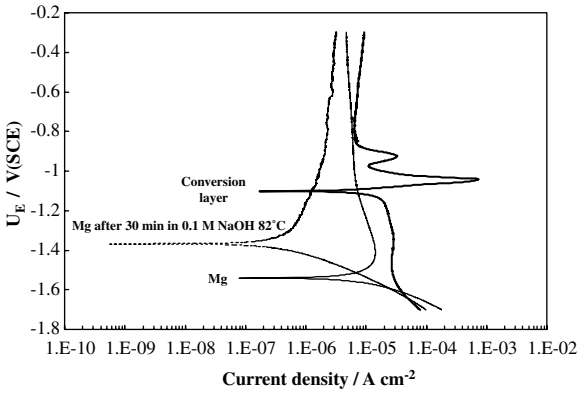

Fig. 6. Polarization curves recorded at 1 mV s^{-1} in 0.1 M NaOH at room temperature for (a) Mg after mechanical cleaning, (b) Mg after mechanical cleaning and 30 min in 0.1 M NaOH at 82 °C and (c) after conversion in solution no. 1 (30 min at 82 °C).

of a relatively uniform coating on Mg metal. In both cases, the presence of $MgSn(OH)_6$ has been revealed, by XRD analysis, in the conversion layer whilst the possible presence of $Mg(OH)_2$, underlying the coatings grown in both solutions, was left unsolved. Photoelectrochemical investigation was performed on both layers soon after the end of conversion process as well as after ageing in laboratory atmosphere at room temperature after variable elapsed times. All investigations were carried in 0.1 M NaOH solution at pH value near to that of the formation bath (pH = 12).

Figs. 7 and 8 show photocurrent spectra, corrected for the efficiency of the lamp–monochromator system, for Mg electrode coated by conversion layer using solution no. 1 and 2, respectively, polarized at open circuit potential $U_{OC} = -1.15$ V/SCE. U_{OC} was almost the same for samples prepared in both solutions and quite well reproducible for every initial treatment and usually ranging around -1.1 ± 0.1 V/SCE, in very good agreement with the values estimated from the polarization curves (see Fig. 6).

The optical band gap value was derived according to the equation:

$$(I_{ph}h\nu) = \text{const}(h\nu - E_g^{opt})^n \tag{1}$$

where $n = 2$ by assuming indirect optical transitions [13–15]. According to Eq. (1), the extrapolation to zero of the plot $(I_{ph}h\nu)^{0.5}$ vs $h\nu$ allows to get the E_g^{opt} value which was quite near for both samples and equal to 3.00 ± 0.1 eV (see inset of Figs. 7 and 8). The photocurrent is cathodic on the whole range of wavelengths at this potential, as evidenced by the phase of the photocurrent signal in chopped light lock-in experiments as well as by looking to the change of the total current in switching on–off the light impinging on the electrode surface.

As for the photocurrent spectra we like to stress that, at U_{OC}, fresh specimen converted in solution no. 1 displayed higher value of photocurrent with respect to the

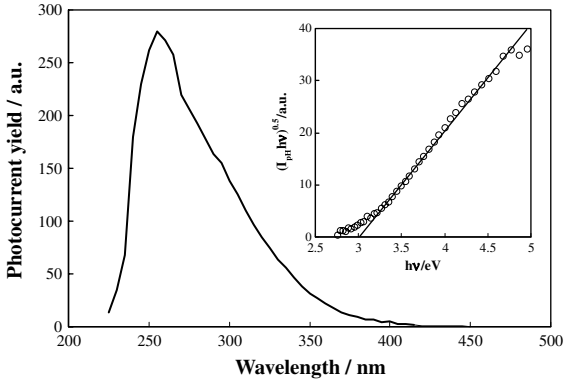

Fig. 7. Photocurrent spectrum corrected for the photon emission of the light source recorded for chemical conversion layer on Mg (30 min in solution no. 1 at 82 °C after mechanical treatment and pickling) at −1.15 V/SCE in 0.1 M NaOH. Inset: determination of the optical band gap by assuming indirect optical transitions.

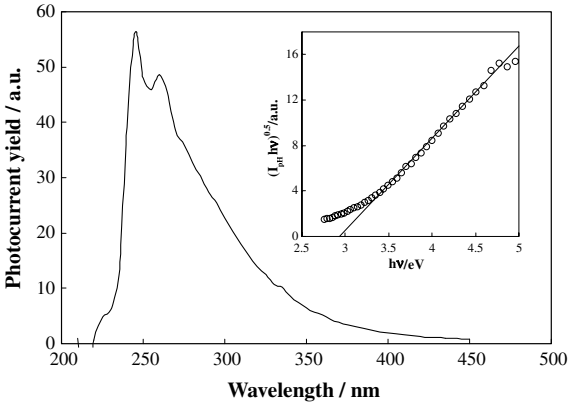

Fig. 8. Photocurrent spectrum corrected for the photon emission of the light source recorded for chemical conversion layer on Mg (60 min in solution no. 2 at 90 °C after mechanical treatment and pickling) at −1.15 V/SCE in 0.1 M NaOH. Inset: determination of the optical band gap by assuming indirect optical transitions.

sample converted in solution no. 2. Regardless of conversion solution usually a tailing at longer wavelengths was observed at U_{OC}. Slightly higher E_g values were recorded, obviously, in the presence of a short tailing (compare Figs. 7 and 8).

The photocurrent spectra recorded at various potentials (both cathodic and anodic with respect to U_{OC}) exhibited also a significant absorption in the region of low energies (long tail). In the case of cathodic photocurrent, the possible onset of an internal electron photoemission process (from the metallic substrate to the conduction band of coating layers) must be taken into account, whilst in the presence of

very thin insulating high band gap material also an external electron photoemission process becomes possible.

In the case of external photoemission processes (tunnelling of electrons through the film to the solution), the threshold energy can be determined according to the so-called 5/2 power law:

$$I_{ph} \propto (h\nu - h\nu_0 - eU_E)^{5/2} \tag{2}$$

where U_E is the applied potential against a reference electrode and $h\nu_0$ is the photoelectric threshold at $U_E = 0$. According to this law, a linear dependence on electrode potential, with a slope of 1 eV/V [13–15], is expected for the external photoemission threshold. Such a linear dependence was not observed so that this type of processes can be excluded as a source of the tailing.

In the hypothesis of internal photoemission, the Fowler law is assumed to hold:

$$I_{ph} = \text{const}\,(h\nu - E_{th})^2 \tag{3}$$

where E_{th} is the internal photoemission threshold energy, which can be obtained from $I_{ph}^{0,5}$ vs $h\nu$ plots [13–15]. According to this in Fig. 9, we report the photocurrent spectrum at $U_E = -1.05$ V/SCE in the tail region and the Fowler plot (see inset) for a sample converted in solution no. 1 for 30 min. An energy threshold value of 1.60 eV can be estimated according to Eq. (3). By polarizing the electrode at different potentials, but in a range where cathodic photocurrent was recorded at any wavelength, internal photoemission threshold values of about 1.65 ± 0.1 eV were determined regardless of conversion solution and time of immersion. This value is much lower than that obtained in the case of non-converted Mg electrodes, immersed in NaOH solution at 82 °C for different immersion times and under similar cathodic polarization [16], showing an internal photoemission threshold of about 2.3 ± 0.1 eV. Such a large difference in the threshold values suggests that the photocurrent action

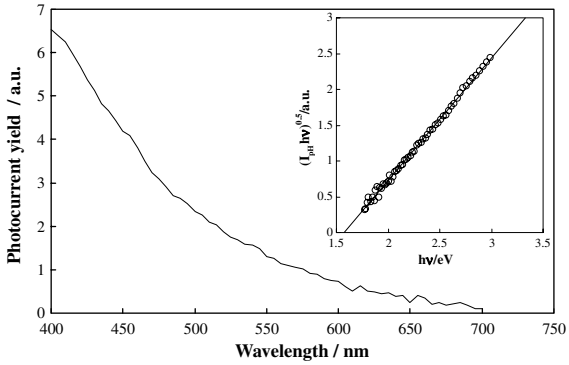

Fig. 9. Photocurrent spectrum corrected for the photon emission of the light source recorded for chemical conversion layer on Mg (30 min in solution no. 1 at 82 °C after mechanical treatment and pickling) at $U_E = -1.05$ V/SCE in 0.1 M NaOH. Inset: determination of the threshold energy according to Fowler law.

spectrum of Fig. 9 could be due to an internal electron photoemission process from the metallic substrate to the conduction band of $MgSn(OH)_6$ conversion layer having insulating-like properties. The possible presence of a very thin (<3–4 nm) $Mg(OH)_2$ layer, underlying the mixed hydroxide, should be still compatible with a process of internal electron photoemission from Mg metal to the conduction band of $MgSn(OH)_6$. We will come back shortly to this point in the following.

To verify the effect of light and applied potential on the photoelectrochemical properties of the conversion layer, photocurrent spectra at various values of U_E have been recorded starting from the corrosion potential. By polarizing the electrode at potential more cathodic than U_{OC}, usually a slightly decrease of the E_g^{opt} value was observed owing to the increase of photocurrent tailing attributed to the presence of an internal electron photoemission process (see above). By increasing the electrode potential in the anodic direction different behaviour could be observed for different electrodes showing almost similar corrosion potential and initial E_g^{opt} value.

When the applied potential moves from U_{OC} towards the anodic direction, the intensity of the photocurrent initially diminishes at any wavelength. Starting from potentials equal or slightly more anodic than −0.5 V/SCE, a sudden change of the photocurrent phase angle against wavelength is noticed, corresponding to the onset of an anodic photocurrent in the region of high energies. From the long wavelengths region, where a still cathodic photocurrent is measured (see Fig. 10), an almost constant cathodic photoemission threshold at around 1.65 ± 0.1 eV is derived.

By increasing the polarizing voltage in the positive direction, a potential value is reached where the entire photocurrent spectrum becomes anodic. When this occurred two band gap values at high and lower photon energy were derived. This potential value changes very much (about 1 V) depending less from the details of the electrode preparation and more from its electrochemical history. According to this although the E_g^{opt} value derived from high-energy region was always accessible at not too high anodic potentials ($U_E \geqslant -0.1$ V/SCE), the low-energy gap was not always accessible until very anodic potentials ($U_E \geqslant 1.0$ V/SCE) were reached.

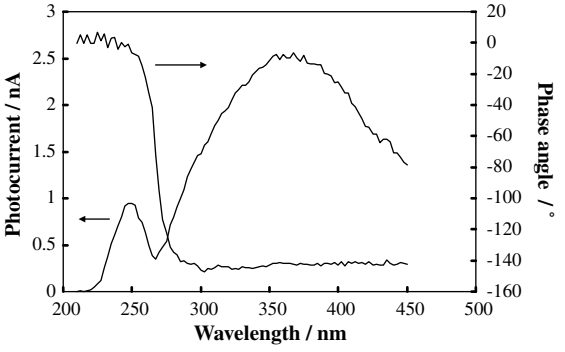

Fig. 10. Raw photocurrent spectrum and phase angle for chemical conversion layer on Mg (30 min in solution no. 1 at 82 °C after mechanical treatment and pickling) at $U_E = 0.0$ V/SCE in 0.1 M NaOH.

When this occurred the two band gap values, although not well reproducible, did not differ too much from those derived in Fig. 12.

In Fig. 11, we report the raw photocurrent spectra for a Mg electrode coated with a conversion layer formed for 30 min in solution no. 1, at three different potentials and after about 12 h of ageing in air at room temperature. When the applied potential moves towards anodic direction the intensity of photocurrent spectrum diminishes and at about −0.1 V/SCE it becomes anodic (see also Fig. 12) at any wavelength, whilst no cathodic photocurrent tailing at longer wavelengths (see Fig. 10) is now observed.

From cathodic photocurrent spectra of Fig. 11, at $U_E = -1.40$ V/SCE and −1.05 V/SCE, an almost constant E_g^{opt} value around 2.90 ± 0.1 eV was derived for indirect optical transitions, whilst at more anodic potentials ($U_E = -0.1$ V/SCE), where only anodic photocurrent was recorded, the spectra displayed different features. This is clearly evidenced in Fig. 12 where the photocurrent spectrum at −0.1 V/SCE, corrected for lamp emission, is reported. As shown in the inset, the $(I_{ph}h\nu)^{0.5}$ vs $h\nu$ plot exhibits now two extrapolation regions. From the region of high energies an optical band gap of about 4.22 eV was determined whilst a second extrapolation, at lower photon energy, gives an E_g^{opt} value around 3.15 eV (see inset in Fig. 12). Almost identical band gap values were also measured at higher anodic electrode potential ($U_E = +0.1$ V/SCE). The value of band gap obtained from the extrapolation of the high-energy region is very close to that reported for anodically grown $Mg(OH)_2$ [14]. As for the second extrapolation, at lower photon energy ($E_g^{opt} = 3.15$ eV), such a value appears very close to that obtained from cathodic photocurrent spectra recorded at very cathodic potentials (see Figs. 7 and 8) and attributed to the presence of $MgSn(OH)_6$ phase.

According to these experimental results it may be suggested that, in this range of potentials, the photocurrent at high photon energy is mainly due to optical

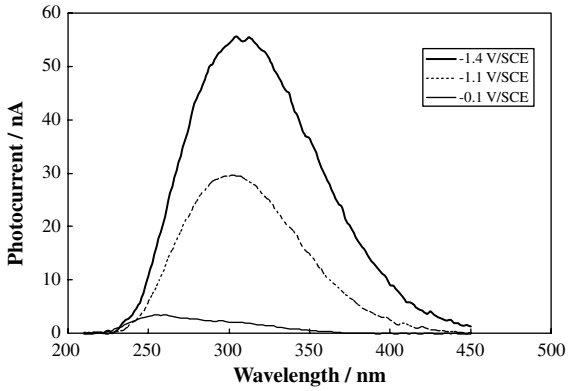

Fig. 11. Photocurrent spectra, not corrected for photon efficiency recorded in 0.1 M NaOH for Mg electrode coated with conversion layer formed in solution no. 1 for 30 min at 82 °C and aged in air for 12 h at room temperature, polarized at various potentials.

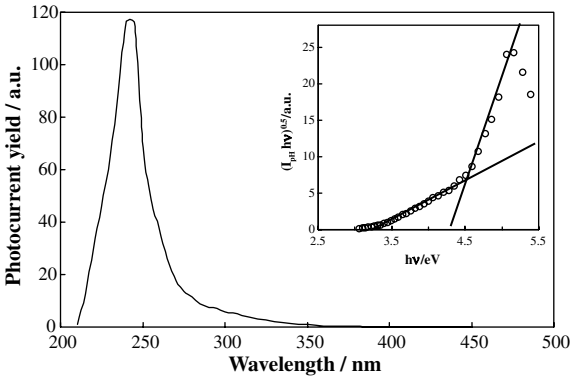

Fig. 12. Photocurrent spectrum corrected for the photon emission of the light source recorded for chemical conversion layer on Mg (30 min in solution no. 1 at 82 °C after mechanical treatment and pickling, aged in air for 12 h at room temperature) at −0.1 V/SCE in 0.1 M NaOH. Inset: determination of the optical band gap assuming indirect optical transitions.

transitions from the valence band to the conduction band of a magnesium hydroxide layer having a band gap of 4.25 ± 0.1 eV.

The attribution of a lower energy gap to the presence of insulating $MgSn(OH)_6$ compound, initially suggested on the basis of XRD data, is further supported by the photoelectrochemical behaviour of Fig. 12. In fact, the almost equal optical band gap values derived from the anodic and cathodic photocurrent spectra, as well as the value of the internal electron photoemission threshold, roughly equal to half the estimated band gap value of mixed hydroxide, strongly support the hypothesis of formation of an insulating layer on the surface of magnesium electrode after immersion in stannate solution.

Analogous findings have been reported in the literature [17] for insulating passive films on bismuth thinner than the stannate conversion layer. However, very low values ($\leqslant 10^3$ cm^{-1}) of light absorption coefficient for under-band gap photon energies are common and could account for the presence of electron photoemission at the substrate/mixed hydroxide interface.

In order to have further information on the photoelectrochemical properties of conversion layers, we recorded photocurrent vs applied potential, by irradiating the electrodes at various constant wavelengths, starting from the U_{OC} and changing the potential in anodic direction at a sweep rate of 5 mV s^{-1}. In Fig. 13, we report the photocurrent vs potential curves at three different wavelengths showing a very asymmetrical behaviour with larger cathodic photocurrent values and much smaller, almost constant, anodic photocurrent especially at longer wavelengths. The values of the inversion photocurrent potential, V_{inv}, shown in Table 2 are relatively scattered but a value close to −0.54 V/SCE or a more cathodic one is a reasonable estimate of such a parameter.

After experiments of Fig. 13, the measured corrosion potential of the electrode was slightly nobler ($U_{OC} = -1.04$ V/SCE), the photocurrent values at any wavelengths

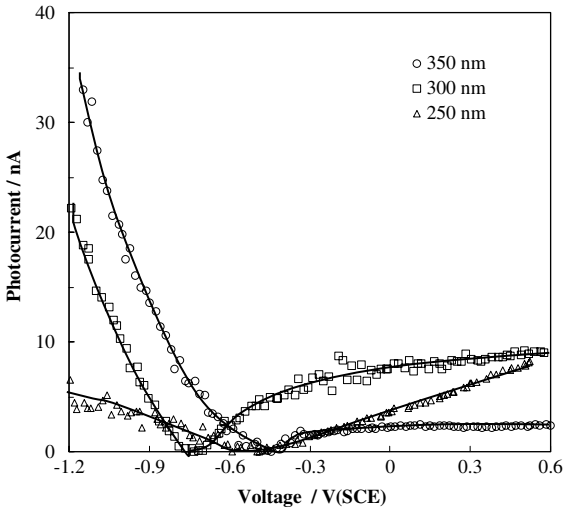

Fig. 13. Photocurrent vs potential for Mg electrode coated by chemical conversion layer formed in solution no. 1 for 30 min at 82 °C recorded in 0.1 M NaOH by irradiating the electrode at different wavelengths ($v_{scan} = 5$ mV s^{-1}).

Table 2
Inversion potential, V_{inv} obtained from I_{ph}–U_E curves, relating to Mg electrode coated by chemical conversion layer grown in solution no. 1 (30 min at 82 °C), recorded by irradiating the electrode at different wavelengths in 0.1 M NaOH

λ, nm	V_{inv}, V/SCE
250	−0.57
300	−0.54
350	−0.73

were sensibly smaller whilst the value of the indirect optical band gap measured at the new U_{OC} remained almost unchanged ($E_g^{opt} = 3.00$ eV).

Analogous experiments on a pure Mg electrode, immersed for 30 min in a solution at pH = 12.5, showed very different behaviour. In fact, a much more anodic inversion photocurrent potential ($V_{inv} \geqslant -0.24$ V/SCE) and almost symmetrical anodic and cathodic photocurrent branches (see Fig. 14) were observed. A more detailed analysis of the photoelectrochemical behaviour of passivated Mg electrodes will be presented in a future paper.

In order to understand the photocurrent behaviour on the anodic side of the photocharacteristics displayed in Fig. 13 different hypotheses can be suggested: (a) the presence of a thin $Mg(OH)_2$ layer underlying the mixed magnesium–tin hydroxide; (b) slow kinetics of photo-holes transfer at the mixed hydroxide/electrolyte interface. According to point (a), a large offset (about 1 eV) in the conduction band of the heterojunction $Mg(OH)_2/MgSn(OH)_6$ can be assumed by considering the difference

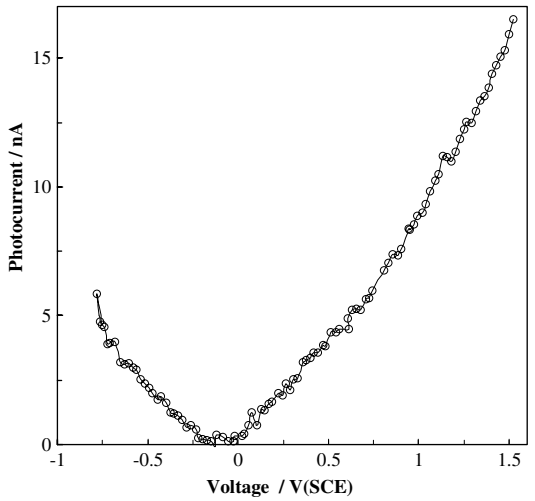

Fig. 14. Photocurrent vs potential Mg electrode after 30 min in 0.1 M NaOH at 82 °C, recorded by irradiating the electrode at 250 nm ($v_{scan} = 5$ mV s^{-1}).

in the band gap values of the two phases (see Fig. 15). This would originate a large recombination, at the $Mg(OH)_2/MgSn(OH)_6$ inner interface, of thermalized photocarriers under anodic polarization. However, the thickness of $Mg(OH)_2$ layer should be not too high in order to make possible the tunnelling of photo-emitted electrons under cathodic polarization.

In the hypothesis (b), the $MgSn(OH)_6$ phase is electrically connected to the underlying metal surface but a strong recombination process is now occurring at the mixed hydroxide/electrolyte interface owing to a very slow kinetics of reaction between the photogenerated hole and the reduced species in solution or at the surface layer. If we

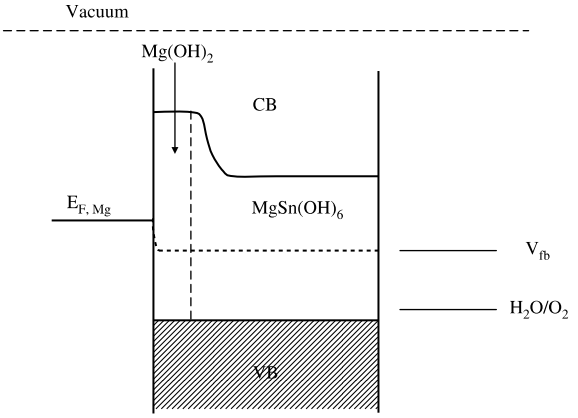

Fig. 15. Schematic diagram of substrate/$Mg(OH)_2/MgSn(OH)_6$/electrolyte interface.

assume that anodic photocurrent is related to the photo-oxidation of the water molecules the small energy distance, if any (see Fig. 15) between E_V and redox level of H_2O/O_2 couple in solution should favour the strong recombination at this interface. The kinetics of the oxygen evolution reaction as well as of layer oxidation are expected to be quite slow. Further investigations on these aspects are necessary before reaching a final conclusion.

In discussing the photoelectrochemical results, we have tacitly assumed that the optical band gap values measured on the Mg electrode after chemical conversion in stannate bath pertain to $Mg(OH)_2$ ($E_g = 4.25$ eV) and to $MgSn(OH)_6$, which are both well-known crystalline hydroxides [18]. Although such an identification has been made indirectly on the basis of XRD patterns and/or thermodynamic consideration we would like to mention that as for the identification of mixed hydroxide $MgSn(OH)_6$, the possibility exists for use of PCS for an "in situ" identification of such mixed hydroxide.

In previous works [14,19], we have proposed a correlation between the band gap of hydroxide and the difference of electronegativity between cation and anion constituents according to the following equation:

$$E_g = A(\chi_M - \chi_{OH})^2 + B \ (\text{eV}) \tag{4}$$

where $A = 1.21$ and $B = 0.90$ for s,p-metal hydroxides, χ_M nd χ_{OH} are respectively the Pauling electronegativity parameter of the metallic cation and of the anion. By assuming for OH^- a value of $\chi_{OH} = 2.85$, obtained by the arithmetic average between the value of hydrogen (2.2) and that of oxygen (3.5) in the Pauling scale, it has been shown that it is possible to correlate a number of optical band gap values of hydroxide of s,p-metal (as well as of d-metal hydroxides by using different A and B values) according to Eq. (4).

By following a procedure, analogous to that followed for mixed oxides [14], it is possible to extend the previous correlation to mixed hydroxides if we introduce in Eq. (4) an average cationic electronegativity parameter. This last parameter has been defined as:

$$\chi_{av} = x_A\chi_A + x_B\chi_B \tag{5}$$

where x_A and x_B represent the atomic fraction of metals A and B in the mixed hydroxide, while χ_A and χ_B are the respective electronegativity parameter. According to Eq. (5), an average cationic value $\chi_{av} = 1.5$ is obtained for $MgSn(OH)_6$ compound, while by using Eq. (4) a band gap value equal to 3.1 eV is obtained for $MgSn(OH)_6$. This result is in very good agreement with the values of band gap reported in Figs. 7, 8 and 10 and it lends further support to the interpretation of PCS data previously described.

4. Conclusions

It has been shown by using both in situ and ex situ methods that a conversion layer of mixed magnesium and tin hydroxides is formed on magnesium metal by

immersion in aqueous stannate baths at high temperature. The morphology and kinetics of growth of the layer change with changing the bath composition.

The PCS study suggests the formation of an insulating mixed hydroxide covering the surface of magnesium hydroxide. By using a previously proposed correlation, the value of measured band gap at very cathodic potentials, as well as at more anodic ones but at lower photon energies, agrees with the hypothesis of formation of a mixed $MgSn(OH)_6$ hydroxide.

Although further studies are necessary before reaching a final acceptance of the proposed correlation for s,p metal hydroxides and to extend it to the case of d metal hydroxide, it is evident that the functional dependence of the band gap values from the difference of electronegativity of the film constituents is a general one. Moreover, the results previously described and recent results on Co hydroxide passive film [20] seem to confirm that as a general rule the hydroxide phases display a smaller band gap than their anhydrous counterpart within some limits previously described [21].

The successful use of an average electronegativity parameter also in the case of mixed hydroxides allows the use of PCS as a quantitative in situ technique for the characterisation of very thin passive films also in the presence of hydroxides formation.

References

[1] J.E. Gray, B. Luan, J. Alloys Comp. 336 (2002) 88.
[2] G. Song, D. St. John, Corros. Sci. 46 (2004) 1381.
[3] E. Gulbrandsen, Electrochim. Acta 37 (1992) 1403.
[4] R. Linstrom, L.-G. Johansson, G.E. Thompson, P. Skeldon, J.E. Svensson, Corr. Sci. 46 (2004) 1141.
[5] G. Song, A. Atrens, D. St. John, J. Nairn, Y. Li, Corros. Sci. 39 (1997) 855.
[6] G. Song, A. Atrens, D. St. John, X. Wu, J. Nairn, Corros. Sci. 39 (1997) 1981.
[7] E. Gulbrandsen, J. Tafto, A. Olsen, Corros. Sci. 34 (1993) 1423.
[8] G. Baril, N. Pebere, Corros. Sci. 43 (2001) 471.
[9] M.A. Gonzales-Nunez, C.A. Nunez-Lopez, P. Skeldon, G.E. Thompson, H. Karimzadeh, P. Lyon, T.E. Wilks, Corr. Sci. 37 (1995) 1763.
[10] H. Huo, Y. Li, F. Wang, Corros. Sci. 46 (2004) 1467.
[11] M.A. Gonzales-Nunez, P. Skeldon, G.E. Thompson, H. Karimzadeh, Corrosion 55 (1999) 1136.
[12] M. Pourbaix, Atlas of Electrochemical Equilibria in Aqueous Solutions, Pergamon Press, Oxford, 1966.
[13] F. Di Quarto, S. Piazza, C. Sunseri, Curr. Topics Electrochem. 3 (1994) 357.
[14] F. Di Quarto, C. Sunseri, S. Piazza, M. Santamaria, in: H.S. Nalwa (Ed.), Handbook of Thin Films, vol. 2, Academic Press, San Diego, 2002, p. 373.
[15] U. Stimming, Electrochim. Acta 31 (1986) 415.
[16] R. Masi, L. Anicai, M. Santamaria, F. Di Quarto, in preparation.
[17] L.M. Castillo, L.M. Peter, J. Electroanal. Chem. Interf. Electrochem. 146 (1983) 377.
[18] F.S. Galasso, in: Structure and Properties of Inorganic Solids, Pergamon press, Oxford, 1970, p. 132, and 168.
[19] F. Di Quarto, M.C. Romano, M. Santamaria, S. Piazza, C. Sunseri, Russ. J. Electrochem. 36 (2000) 1203.
[20] M. Santamaria, E. Adragna, F. Di Quarto, Electrochem. Solid-State Lett. 8 (2005) B12.
[21] F. Di Quarto, M. Santamaria, C. Sunseri, in: P. Marcus, F. Mansfeld (Eds.), Analytical methods for Corrosion Science and Engineering, Taylor and Francis Group, Boca Raton, 2006, p. 697 (Chapter 18).